Vision-based hexagonal image processing using Hex-Gabor

Article *in* Signal Image and Video Processing · February 2014
DOI: 10.1007/s11760-012-0293-5

2 authors:

S. Veni
Amrita Vishwa Vidyapeetham

Narayanankutty K.A.
Amrita Vishwa Vidyapeetham

SIViP (2014) 8:317–326
DOI 10.1007/s11760-012-0293-5

ORIGINAL PAPER

Vision-based hexagonal image processing using Hex-Gabor

S. Veni · K. A. Narayanankutty

Received: 3 June 2011 / Revised: 2 February 2012 / Accepted: 3 February 2012 / Published online: 22 February 2012

Abstract About 97% receptive field of the neurons is very closely described as 2D Gabor wavelet and it is mostly suitable for vision system modeling. Immense work is available on texture information, especially for rectangular structures. However, there is a little work in recognizing minute details in an image on hexagonal structure by either interpolation or enhancement. In this work, the two important operations of biological visual system such as enhancement and interpolation are performed using the Hex-Gabor process. It is possible to obtain an error-free image at sigma = 2/pi using the proposed Hex-Gabor process and the significance of this sigma value is proved. For the performance analysis standard reflected images and X-ray images are considered.

Keywords Hexagonal image processing · Hex-Gabor filter · Image enhancement · Interpolation

1 Introduction

There exist three possible regular tessellation schemes namely the tessellations with squares, hexagons, and triangles. Hexagonal Image Processing (HIP) with an effort to enhance the quality of the image is performed in this work. The primary motivation behind using hexagonal pixel grid is that the retina of the eye closely resembles a hexagonal grid space. The possibility of using a hexagonal structure to represent digital images and graphics has been studied by many researchers [1–3]. Using hexagonal grid, wider spectra can be sampled without aliasing with the same number of pixels or less pixel than using square grid.

The use of hexagonal grid is fettered by its pixel arrangement. In the hexagonal structure, the pixels are no longer arranged in rows and columns. In order to take the advantages of the special structure of hexagonal grid and store hexagonal images data, several addressing schemes and coordinate systems have been proposed [4,5]. In the past years, there had been many attempts in representing hexagons in the regular square lattice or in a Spiral Addressing Scheme (SAS) [6,7]. Regular geometry is only kept in the case of SAS; however, processing such pseudo lattices gave rise to better results compared with square lattices.

For a 2-D image, it is customary to apply the B-splines successively in 1-D along horizontal and vertical directions on rectangular lattices [8–10]. Hex-splines [11,12] are proven for their quality for image interpolation by re-sampling techniques on hexagonal lattices. Hex-splines were already successfully applied to some printing applications [11]. Hex-spline by Petrou [13] proposed bio-inspired algorithm for invariant image reconstruction from irregular samples and used linear B-splines with control points on hexagonal grids.

Biological visual system can be modeled as a cascade of sub filters covering the major processing layers found in mammal visual systems from photoreceptors over ganglion cells in the retina up to simple cells in the primary visual cortex [14]. The orientation selective receptive fields can be modeled by Gabor filters which are products of sinusoidal gratings and Gaussian envelopes. Previous studies have shown that Gabor filters closely resemble experimentally measured receptive fields in the visual cortex [15] and have been widely used to model the response of visual cortical neurons. One of the important features of the Gabor filter is

S. Veni (✉) · K. A. Narayanankutty
Department of Electronics and Communication Engineering, Amrita Vishwa Vidya Peetham, Ettimadai, Coimbatore 641112, Tamil Nadu, India
e-mail: s_veni@cb.amrita.edu

K. A. Narayanankutty
e-mail: ka_narayanankutty@yahoo.com

that they can be easily tuned to different center frequencies, dilations, and orientations [16–19].

The standard definition of a two-dimensional Gabor function used in this work is according to Manjunath and Ma [19]. A two-dimensional Gabor function $g(x, y)$ and its Fourier transform $G(u, v)$ can be written as:

$$g(x, y) = \left[\frac{1}{2\pi\sigma_x\sigma_y}\right]\exp\left[-\frac{1}{2}\left[\frac{x^2}{\sigma_x^2}+\frac{y^2}{\sigma_y^2}\right]+2\pi jFx\right] \quad (1)$$

In the frequency domain,

$$G(u, v) = \exp\left\{-\frac{1}{2}\left[\frac{(u-F)^2}{\sigma_u^2}+\frac{v^2}{\sigma_v^2}\right]\right\} \quad (2)$$

where $\sigma_u = \frac{1}{2\pi\sigma_x}$ and $\sigma_v = \frac{1}{2\pi\sigma_x\sigma_y}$
while σ_x and σ_y are the standard deviations of the elliptical Gaussian along x and y axes and F is the radial frequency [Eq. (1)].

Our previous work includes Gabor functions for interpolation on hexagonal Lattice [20] and image enhancement of medical images using Gabor filter bank on hexagonal sampled grids [21]. Half pixel shift method was used in order to mimic the hexagons. In this work, Hex-Gabor kernel/Hex-Gabor is designed by adding the responses at three orientations ($0°, 60°,$ and $120°$) of the hexagonal grid. The kernel is used for the image enhancement and interpolation applications. The Features of Hex-Gabor are explained in Sect. 2. In order to perform a comparative study with Hex-Gabor, the interpolation using Hex-spline which is proposed by Van De Ville et al. [11] is modeled using MATLAB.

The paper is organized as follows. Section 2 deals with features of Hex-Gabor kernel. In Sect. 3, image enhancement and interpolation operations using Hex-Gabor are addressed. Implementation results with respect to Hex-Gabor are explained in Sect. 4. In Sect. 5, enhancement of Reflected and X-ray images using Hex-Gabor and its implementation results are elaborated. Conclusions are given in Sect. 6.

2 Overview of Hex-Gabor and its features

Image reconstruction through interpolation is a routine task during processing all transformation that is made on an image. Such transformations include scaling, rotation, registration, and edge detection. A low-pass filter and high-pass filter may be used to enhance surface information and edge information, respectively. When we put kernels on image pixel locations and add, it enhances the image and also facilitates interpolation. A modulated wave filter is more effective in edge enhancement and texture than a unipolar narrow filter at higher resolution (can also be called as high-pass filter as in a Gaussian wave). In regular lattice isotropic kernels are necessary, but for unequal pixel distances directional and orthogonal direction filtering are important. This explains the reason for combining the responses of the filter-banks. Hence, three orientations Hex-Gabor kernel is designed by adding the responses of $0°, 60°,$ and $120°$ and the resultant kernel is obtained. It was found that only an optimum value of sigma (2/pi) made a visually error-free image. It was also noted that minor corrections are required at the receding end of the kernel by windowing. It is clearly evident that sigma (σ in Eq. 1) values have to be kept same in all directions. However, only the specific value could yield a good result. In scattered images like X-rays, the contribution to intra-pixel information is not very obvious, and hence this was attempted. Different sigma values enhanced different depth information in such images.

Some of the main features of Hex-Gabor can be summarized as follows: (i) It is capturing intra-pixel information only because it is filtered through a 2D hex base. Conventional Gabor filtering in square lattice does not do this, because it only considers pixels along a line whether it is horizontal, vertical, or along axes in hex domain. (ii) Hex-Gabor is considering the intra-pixel distances and directions of adjacent pixels in a regular lattice also. (iii) At sigma value 2/pi the kernel is isotropic, and nonlinear. This enabled filtering that would enhance the image edges and would retain smooth information in any regular lattice. (iv) The resulting kernel can be used in rectangular lattice and we could obtain same results as that has been achieved with hexagonal image processing. This shows the importance of considering components in the orthogonal directions. (v) It also shows that if this is considered, even a shift from regular hexagonal lattice of the retinal elements could be suitably compensated. The results in this work also show how finer details are visualized by this sigma selection by the eye. For sigma values more than 2/pi, (Eq. 1), the kernel is not unipolar. (vi) The isotropy of the Hex-Gabor kernel is lost when sigma exceeds 2/pi, and smooth filtering qualities are lost at this condition. To demonstrate this, the shapes of the kernels are displayed below (Fig. 1) for sigma = 1/pi, 2/pi, and 3/pi, respectively. (vii) Filtering quality reduces substantially for a slight increase/decrease in the value of sigma after 2/pi. (viii) While using kernels for image enhancement it generates continuous image surface enabling interpolation. In addition to the fact that Gaussian kernels are suitable for this purpose, a compact support is also ensured in this method. (ix) Hex-Gabor is doing a nonlinear filtering [22] operation using an isotropic kernel which is shown in Fig. 2. (x) Another interesting property of Hex-Gabor is the data are nearly fitting with cubic B-spline data (Fig. 3) at sigma = 2/pi (as per its well-known equation defined in [23,24]) as

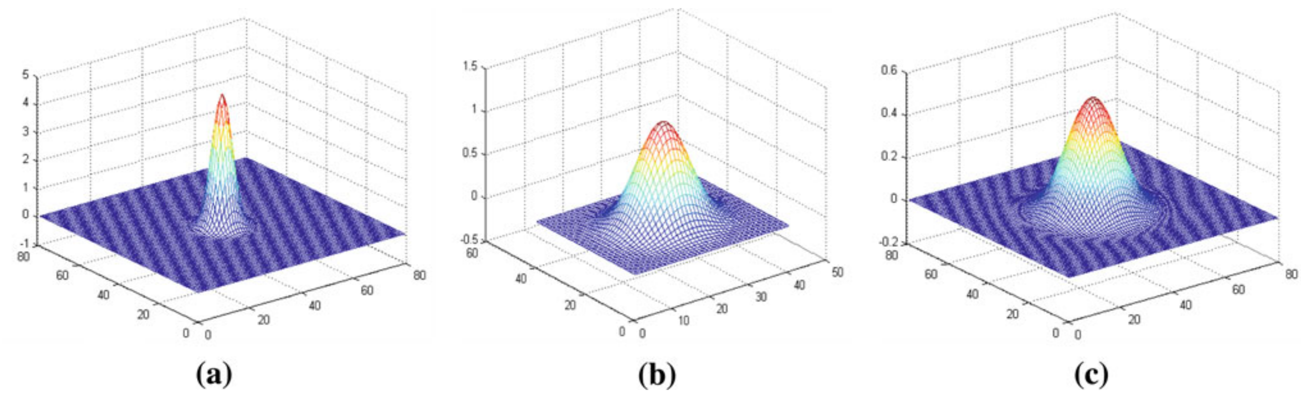

Fig. 1 Hex-Gabor kernels at different sigma values. **a** Sigma = 1/pi, **b** sigma = 2/pi, **c** sigma =3/pi

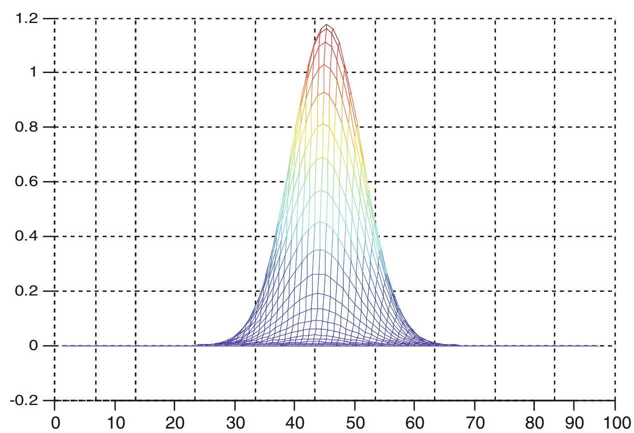

Fig. 2 Hex-Gabor kernel with details of absolute values at sigma = 2/pi

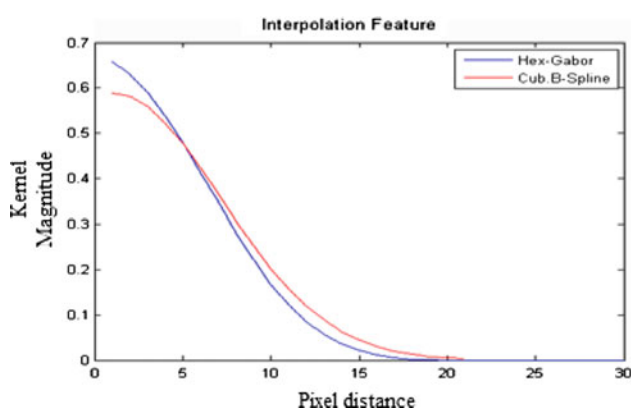

Fig. 3 Comparison of Hex-Gabor data and cubic B-spline data—Horizontal scale pixel distance ×10

$$\beta^3(x) = \begin{cases} \frac{2}{3} - \frac{1}{2}x^2(2-x) & 0 \leq |x| < 1 \\ \frac{1}{6}(|2-x|)^3 & 1 \leq |x| < 2 \\ 0 & 2 \leq |x|\,. \end{cases} \tag{3}$$

(xi) Gradient is computed by taking difference between the absolute values of the Hex-Gabor at sigma = 2/pi as shown

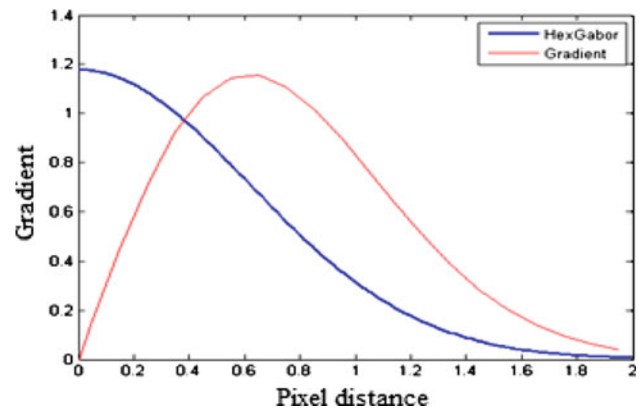

Fig. 4 Computation of gradient with respect to pixel distance

in Fig. 4. Gradient is found to be maximum at 0.636 (2/pi). (xii) The absolute values of the kernel (Fig. 2) are as follows:

Absolute values =1.1781, 1.1627, 1.1176, 1.0464, 0.9542, 0.8475, 0.7331, 0.6176, 0.5068, 0.4049, 0.3151, 0.2388, 0.1762, 0.1266, 0.0885, 0.0603, 0.0400, 0.0258, 0.0162, 0.0099
Valueoforiginalpixel = 1.1781 + 3 × 0.0099 = 1.2078
Interpolated value =3 × 0.4049 = 1.2147, There is no contribution from 4th pixel position. A normalization would correct all values:

3 Hex-Gabor interpolation and enhancement

Image interpolation can be used in image enlargement and local image zooming. Several commonly used interpolation algorithms on rectangular and hexagonal lattices have been suggested by various authors [8–12]. Training of images is done to obtain specific orientation or circular features in an image for the purpose of super resolution [25]. However, no such training is required in Hex-Gabor case as edge enhancement simultaneously takes care of the smooth parts of the image. Gabor filtering methods [26] also tackle the image piecewise along the edges, which deteriorates information along orthogonal directions.

Spline interpolation is used through Hex-splines for the purpose of shear interpolation by earlier workers [11]. Gabor filter is different from splines as it is a modulated basis function. It gathers simultaneously low-pass information through its envelope and high frequency information from modulating wave. This may be used to gather mutual information simultaneously between three neighboring pixels in three directions if intra-pixel information is derived. A Hex-Gabor function is a directional filter function when used separately, but when combined, it is isotropic. Interpolation function may have low-pass characteristic, simultaneously may have edge enhancement characteristic due to its nonlinearity. For an interpolation factor by two, the magnitudes of cubic B-spline and Hex-Gabor are matching (Figs. 3, 4). An interpolation function in a Hex domain (Hex-Bspline-spline used in three directions) could be different from that in square domain (Bspline itself is used in two directions). Hex-Gabor filters as such are suitable for enhancement and interpolation in regular lattices.

3.1 Nonlinear aspect of Gabor filter

When designing two-dimensional nonlinear filters for image processing, one usually imposes an additional requirement that the constructed operator is isotropic with respect to changing the original image's orientation. Nonlinear diffusion processes can be found in many recent methods for image processing and computer vision. In image processing and computer vision, anisotropic diffusion also called Perona–Malik diffusion is a technique aiming at reducing image noise without removing significant parts of the image content, namely edges, lines, or other details that are important for the interpretation of the image. Anisotropic diffusion resembles the process that creates a scale-space where an image generates a parameterized family of successively more and more blurred images based on a diffusion process. Each of the resulting images in this family is given as a convolution between the image and a 2D isotropic Gaussian where the width of the filter increases with the parameter [22]. This diffusion process is a *linear* and *space-invariant* transformation of the original image. Anisotropic diffusion is a generalization of this diffusion process: it produces a family of parameterized images, but each resulting image is a combination between the original image and a filter that depends on the local content of the original image. As a consequence, anisotropic diffusion is a *nonlinear* and *space-variant* transformation of the original image.

The combination kernel obtained through Hex-Gabor is isotropic and nonlinear. This is a favorable condition for edge enhancement. A step further, Kramer's PDE model [28] utilizes both of these more effectively (A comparative result is given in Fig. 12. Similar and/or better results were obtained by the use of Hex-Gabor method in square lattice processing. The results with the Hex-Gabor also support the results of Gabor filter [27] in respect of solution by heat equation, using a negative sign for the Δu where u denotes the image.

3.2 Comparative study of Hex-spline and Hex-Gabor

Foster et al. [30] proved that by defining B-splines with complex exponents, it is possible to construct complex wavelet bases that are tunable in a continuous fashion and that can closely approximate Gabor functions. These extended complex B-splines inherit most of the properties of their classical polynomial counterparts, and that they can generate a variety of multiresolution bases. The basis functions are tunable with respect to two parameters. The real part of the complex exponent (degree) is responsible for the smoothness, whereas the imaginary part induces a one-sided predominance in the frequency domain. This latter property is especially interesting for signal analysis. Chaudhury and Unser [31] constructed a family of complex spline wavelets that resemble the directional Gabor functions proposed by Daugman. Thus, the Hex-Gabor kernel proposed in this work is able to satisfy most of these properties even on the rectangular lattice.

Hex-spline is a family of bivariate, nonseparable spline especially designed for hexagonal lattices. The starting point of the construction is the indicator function of the Voronoi cell, which is used to define the first-order hex-spline in a natural way. Higher-order hex-splines are obtained by successive convolutions [11]. Hex-spline is a framework necessary for the regular hexagonal arrangement, for which another alternative is only the spiral addressing scheme. Therefore, a change of platform was found necessary for utilizing the results in conventional image processing. Hex-spline strategy was used for Gabor filter–based interpolation and the results are included in this work (Sect. 5.3—Fig. 9, Table 3). Hexagonal interpolation may also used to gather mutual information between three neighboring pixels and in three directions of the hexagonal lattice, if intra-pixel information is resulting from directional filtering effects. With the same structure, image enhancement and interpolation were attempted with Hex-Gabor kernel using the three directional filtering.

4 Implementation results of Hex-Gabor

From the results of Fig. 5 below, it is evident that Hex-Gabor is considering the intra-pixel distances and directions of adjacent pixels in any regular lattice. At sigma value 2/pi, the kernel is isotropic, unipolar, and nonlinear (Fig. 5a–d). This enabled filtering that would enhance the image edges and

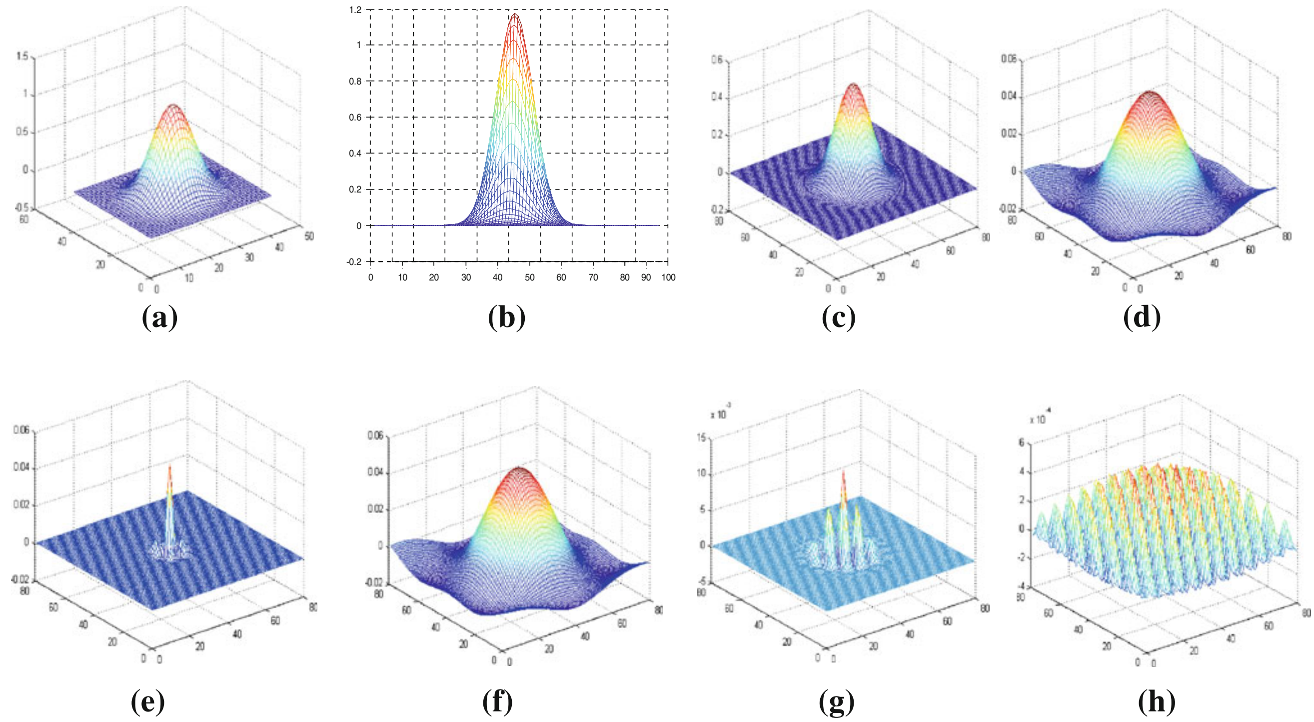

Fig. 5 Plot of Hex-Gabor kernel at different sigma values **a**, **b** sigma = 2/pi (isotropic), **c**, **d** sigma = 3/pi (quasi-isotropic), **e**, **f** sigma = 10/pi (nonisotropic), **g** sigma = 20/pi, **h** sigma = 100/pi

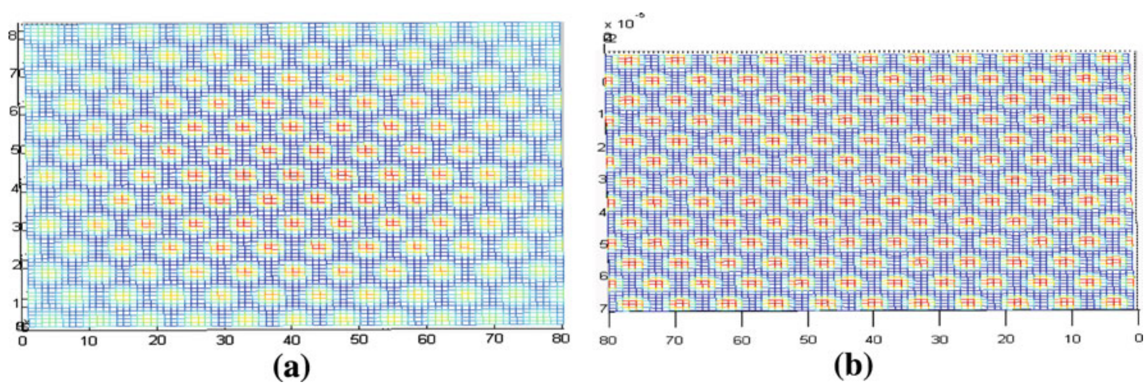

Fig. 6 Hex-Gabor kernel surface at **a** sigma = 100/pi, **b** sigma = 500/pi

would retain smooth information in any regular lattice. The isotropic property is lost if the sigma value exceeds 2/pi as illustrated by Fig. 5e–h.

From the results of Hex-Gabor surface in square lattice, plot for sigma = 100/pi and more (Fig. 6) it is clear that it can produce continuous surface and Gabor profiles as represented in a hexagonal lattice.

5 Enhancement of reflected and X-ray images using Hex-Gabor

Diffusion type of image processing requires that the pixel information in the nearby pixels to be correlated. This is possible in case of normal images. In the X-ray image, intensities in adjacent pixels could be uncorrelated, as it might be coming from an interfering object in the path of X-rays. This is also due to the source of illumination which is not absolutely normal to the photographic plate for this pixel information. The edges and quality of the images can be enhanced by Hex-Gabor for the reflected images and scattered images like X-ray images considered in this work. It was possible to obtain more PSNR value at unique sigma (2/pi) in the case of reflected images. But, it was unsuccessful in enhancing X-ray images with one unique value of sigma. Hence, the range of values from 0.1 to 3 was used for the analysis. Generally, $\sigma_{v0} = 0.75$, $\sigma_{v1} = 1.5$, $\sigma_{v2} = 3.0$ for simple, medium, and large simple cell width, respectively [37].

Table 1 Performance measures of Hex-Gabor kernel filter on mimicking hexagonal grid (half pixel shift) with windowing technique on reflected normal images

Image type	Hex-Gabor response without using window			Hex-Gabor response with Hanning window		
	PSNR	MSE	Computation time (in s)	PSNR	MSE	Computation time (in s)
Wood	52.89	0.3340	3.72	57.54	0.1082	10.27
Lena	54.75	0.2177	3.45	54.99	0.2053	13.33
barbara	54.98	0.2063	3.44	59.75	0.0654	12.22
Peppers	57.76	0.1087	3.36	58.01	0.1028	13.25
MRI	63.29	0.0197	3.87	65.50	0.0183	5.25
Bacteria	53.92	0.2654	4.85	60.89	0.0424	6.81
Pout	52.95	0.3321	3.36	64.58	0.0143	8.21
Testpat	53.38	0.2981	4.52	59.44	0.0587	8.83
Window	56.06	0.1654	3.42	61.88	0.0335	16.98

Various X-ray image enhancement operations were proposed for rectangular lattice such as nonlinear mapping functions [29], Discrete Wavelet Transforms (DWT) [32], canonical correlation-based Kernel Independent Component Analysis (KICA) [33], etc. Our previous work [21] includes processing of medical and X-ray images using three directional Gabor filter on mimicking hexagonal scheme. In this work, an attempt is made to process the enhancement of X-ray images using Hex-Gabor on rectangular grid without using mimicking scheme. Hanning window (Eq. 4) is used to regulate the signal which yields better results. It is seen that a Hanning window requirement is eight times the size of kernel where size of the kernel is $3\sigma(\sigma = 2/\text{pi})$ which gives the best results. It is selected in such a way that the magnitude of the kernel at the second pixel location reduces to almost zero as in the case of B-Spline. The window is expressed as [34],

$$h_k = 0.54 - 0.46\cos\left[\frac{2\pi k}{N-1}\right], \quad 0 \le k \le N. \tag{4}$$

5.1 Image enhancement results of Hex-Gabor on mimicking hexagonal grid

Table 1 summarizes the results of Hex-Gabor on mimicking hexagonal grid (Half pixel shift) using windowing. The half pixel shift method proposed by periasamy [35] is used in this work for performance comparison. Even though there is marginal improvement in PSNR and MSE values, it was possible to obtain good visual appeal on the enhanced image compared with the response without using window. As Hex-Gabor is performing well on true rectangular lattice (discussion in Sect. 2), we are not doing further analysis on this.

5.2 Image enhancement results of Hex-Gabor on true rectangular lattice with windowing technique on reflected images

The Hex-Gabor was tested on true rectangular lattice without using any mimicking scheme and it yields better enhanced image. Some of the results are shown in Fig. 7. The performance is better in terms of PSNR and MSE (Table 2).

The response of the Gabor filter depends on the tuning of the parameter sigma (Eq. 2). To prove the validity of sigma at 2/pi, the response of the Hex-Gabor was tested for the range of sigma values from 0.1 to 3 as mentioned earlier. Figure 8 is the plot of the details shown in the Table 3 (sigma values vs PSNR value—for Barbara image). The parameter sigma = 2/pi yields maximum PSNR value. The Hex-Gabor kernel at this value has also some interesting properties which were mentioned in the Sect. 2. The image quality at other sigma values, both PSNR and visual quality deteriorated substantially. It was noted that the effect of Hex-Gabor is pronounced in other pseudo lattices with this value of sigma, and suboptimal image quality is obtained for three direction operations as in regular hexagonal lattice.

5.3 Implementation issues and algorithm computational complexity

For performance comparison, Hex-spline kernel is modeled using the MATLAB software and applied for image enhancement. Figure 9 illustrates the enhancement results of Hex-spline and Hex-Gabor. From the results, it is evident that Hex-Gabor enhancement yields better visual appeal including edge enhancement. For the objective analysis, three parameters namely PSNR, MSE, and computation time are

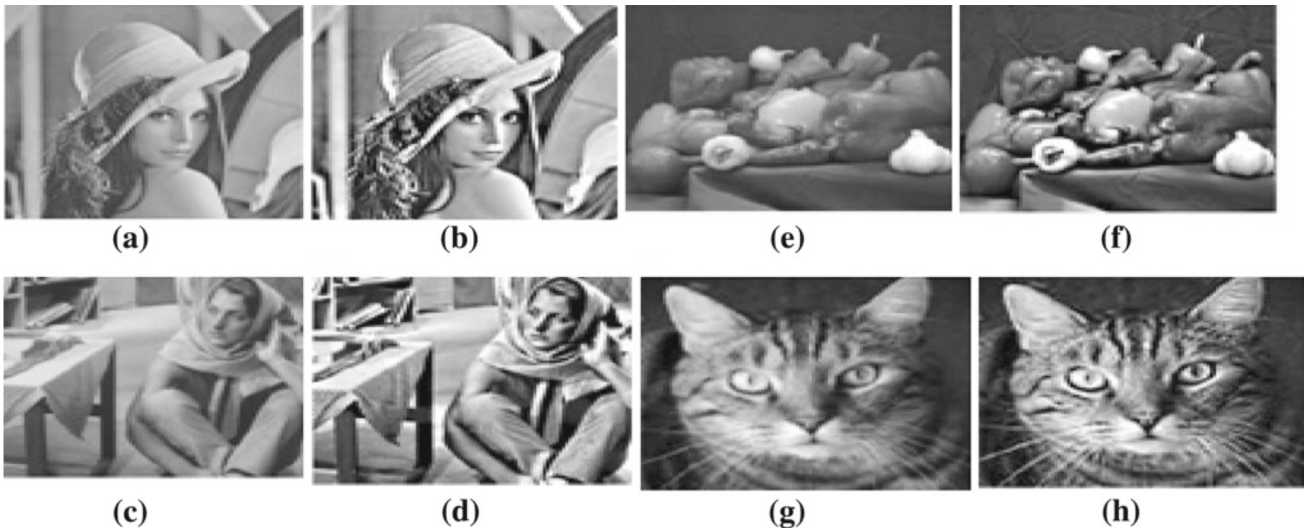

Fig. 7 **a**, **c**, **e**, **g** Original images Lena, Barbara, Peppers, and Cat, respectively. **b**, **d**, **f**, **h** Enhanced images using Hex-Gabor

Table 2 Performance measures of image enhancement using Hex-Gabor on true square lattice with windowing technique on reflected images

Image type	PSNR	MSE	Computation time (s)
Wood	64.83	0.0214	12.27
Lena	65.31	0.0044	14.32
barbara	71.01	0.0064	15.22
Peppers	68.19	0.0013	13.28
MRI	66.43	0.0176	5.36
Bacteria	62.78	0.0378	6.88
Pout	66.58	0.0143	7.21
Testpat	60.44	0.0587	7.83
window	62.88	0.0335	15.98

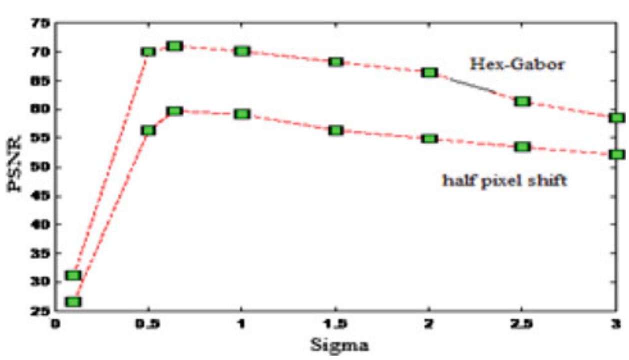

Fig. 8 Plot of sigma versus PSNR for the Barbara image using Hex-Gabor

Table 3 Performance comparison of image enhancement results of Hex-Gabor using half pixel shift and Hex-Gabor for the sigma values from 0.1 to 3 (Barbara image)

	Image type : Barbara.png							
Sigma	0.1	0.5	0.637	1	1.5	2	2.5	3
PSNR (half pixel shift)	26.6	56.3	59.7	59.0	56.4	54.9	54.3	52.1
PSNR (Hex-Gabor)	31.2	69.9	71.0	70.1	68.2	66.5	61.3	58.5

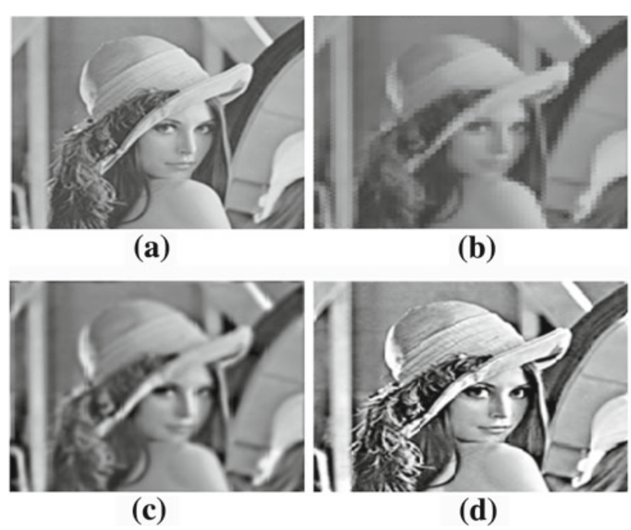

Fig. 9 Comparative study of Hex-spline and Hex-Gabor. **a** Original image, **b** tiling using Hex-spline, **c** enhanced image using Hex-spline, **d** enhanced image using Hex-Gabor

considered (Table 4). Hex-Gabor response is found to be better in terms of more PSNR and less MSE. But, computation time of Hex-Gabor process is marginally increasing because of windowing operation compared with Hex-spline process.

Table 4 Performance comparison of image enhancement results of Hex-Gabor and third-order Hex-spline

Image type	Response of third-order Hex-spline			Response of Hex-Gabor at sigma = 2/pi		
	PSNR	MSE	Computation time (in s)	PSNR	MSE	Computation time (in s)
Wood	55.54	0.2053	4.12	64.83	0.0214	12.27
Lena	53.88	0.2085	5.92	65.31	0.0044	14.32
barbara	57.53	0.1015	5.72	71.01	0.0064	15.22
Peppers	56.88	0.1810	4.25	68.19	0.0013	13.28
MRI	63.56	0.1028	3.98	66.43	0.0176	5.36
Bacteria	59.75	0.0654	5.08	62.78	0.0378	6.88
Pout	64.44	0.0183	4.35	66.58	0.0143	7.21
Testpat	58.04	0.0654	5.37	60.44	0.0587	7.83
Window	60.54	0.0567	4.73	62.88	0.0335	15.98

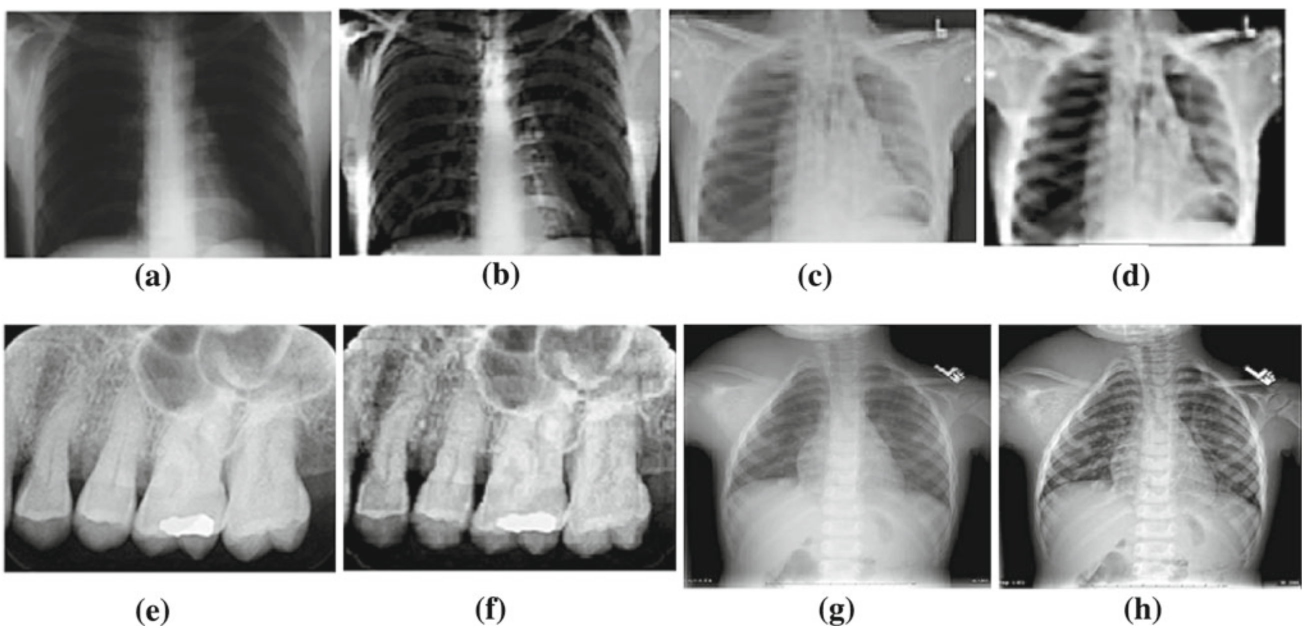

Fig. 10 **a**, **c**, **e**, **g** Original images of chestxray.tif, thumb.jpg, X-ray1.jpg, and X-ray2.jpg, respectively. **b**, **d**, **f**, and **h** Enhanced images using Hex-Gabor [21]

Table 5 Performance comparison of the enhanced images using Hex-Gabor with (i) Half pixel shift approach and (ii) Hex-Gabor on true square lattice (sigma = 2/pi)

Image type	Hex-Gabor response on hexagonal lattice using half pixel shift approach			Hex-Gabor response on true square lattice		
	PSNR	MSE	Computation time (in s)	PSNR	MSE	Computation time (in s)
Chest X-ray	64.296	0.024	6.72	69.30	0.0076	8.87
Thumb	59.452	0.073	2.63	67.88	0.0106	8.91
X-ray1	54.506	0.230	1.56	61.51	0.046	3.26
X-ray2	54.307	0.241	6.23	71.99	0.0041	10.63

5.4 Enhancement of X-ray images using Hex-Gabor filter

Gabor filter models may also be specially parameterized for X-ray images (Fig. 10) considering the optical and interfering characteristics of objects [21]. It was found that different values of sigma gave enhancement of different depth information. The range of sigma values for the scattered images like X-rays varies from 0.5 to 3.

Table 5 summarizes the performance comparison of the enhanced images using Hex-Gabor on (i) Mimicking scheme using half pixel shift approach (ii) true square lattice at sigma = 2/pi. It would not be necessary to use methods like half pixel shift method to get similar results. Because, Hex-Gabor is considering the intra-pixel distances and directions of adjacent pixels in any regular lattice. A set of original and processed images are shown in Fig. 10. Computation time is found to be high for the Hex-Gabor response on true rectangular lattice.

5.5 Comparison of Hex-Gabor results with nonlinear diffusion process and Kramer's PDE model

As discussed in the Sect. 3.1, the nonlinear function of Hex-Gabor $1.1781/(1+(\frac{x}{\sqrt{2}})^2)$ is analyzed and plotted (Fig. 11)

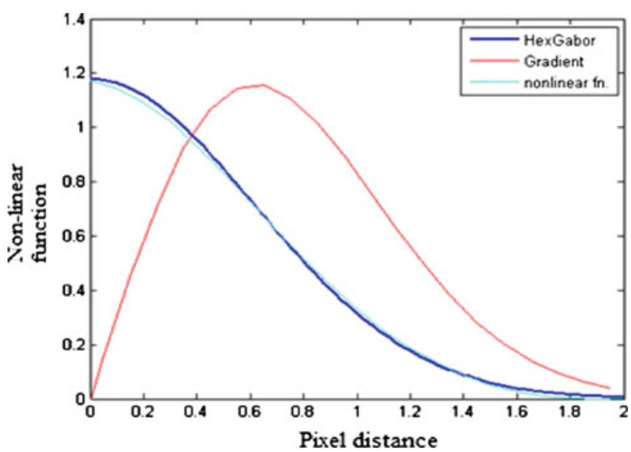

Fig. 11 Nonlinear windowed function $1.1781/(1+(\frac{x}{\sqrt{2}})^2)$) and Hex-Gabor kernel plotted on the same figure

where 1.1781 is the peak absolute value of the Hex-Gabor kernel obtained. The nonlinear function is proved to be the favorable condition for both image interpolation and image enhancement which is evident from the results as discussed in the Sects. 5.2 and 5.4.

Figure 12 shows the comparative results of Kramer's PDE model [28] and Hex-Gabor. The enhanced image obtained using Kramer's PDE model is like a negative image (Fig. 12b). It was possible to get a better quality image including the edges using Hex-Gabor (Fig. 12c) and it can be noticed that soft tissues are enhanced well.

6 Conclusions

Hex-Gabor filter proposed in this work is found to be suitable for enhancement and interpolation. Assuming that all the operations required by human visual system are by Gabor filters in hexagonal domain, it is now established by the results of this work in terms of its perfection to view minutest details and sigma is also tuned for detailed and/or global vision. For normal reflected images it was possible to obtain better results at unique sigma. As X-ray images contain light scattered pixels instead of unique sigma, the range of sigma from 0.5 to 3 was found to satisfy most of the image interpolation/enhancement requirements in terms of visual effects. From the comparative study, the performance of hexagonal grid–based operations using Hex-Gabor was found to be better than the Hex-spline process. Yue Yang and Baoxin [36] proposed nonlinear image enhancement using Gabor filter for digital TV applications in rectangular lattice and image-based kernels are also adopted for high definition TV. Hex-Gabor, therefore, would find much application in high definition TV which can be considered as future work. Isotropy is not destroyed using this method if we choose proper sigma value and it is parallelized. Hex-Gabor is also used in this work for X-ray imaging. It can also be used for the other medical image processing applications.

Fig. 12 **a** Original image, **b** enhanced images using the approaches (**b**) Kramer PDE model-Ref [28] **c** Enhanced image using Hex-Gabor

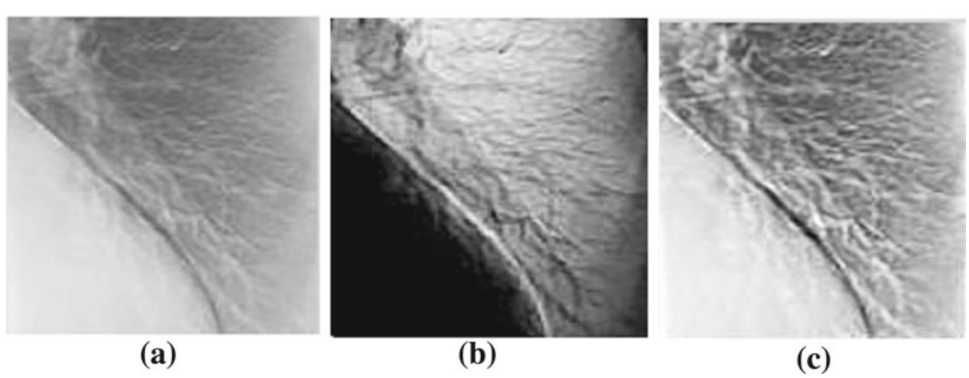

References

1. Kamgar-Parsi, B., Sander, W.A.: Quantization error in spatial sampling: comparison between square and hexagonal pixels. In: Proceedings of the Conference on Computer Vision and Pattern Recognition (CVPR), pp. 604–611 (1989)
2. Vitulli, R.: Aliasing effects mitigation by optimized sampling grids and impact on image acquisition chains. In: Proceedings of the Symposium on Geoscience and Remote Sensing Symposium (IGARSS), pp. 979-981 (2002)
3. Staunton, R.C.: The processing of hexagonally sampled images. J. Adv. Imaging Electron. Phys. **119**, 191–265 (2001)
4. Her, I.: Geometric transformations on the hexagonal grid. In: IEEE Trans. Image Process. **4**(9), 1213–1222 (1995)
5. Hartman, N.P., Tanimoto, S.L.: A hexagonal pyramid data structure for image processing. IEEE Trans. Syst. Man Cybernet. **14**, 247–256 (1984)
6. Sheridan, P.: Spiral Architecture for Machine Vision. University of Technology, Sydney (1996)
7. Wu, Q., He, X., Hintz, T.: Virtual spiral architecture. In: Proceedings of the International Conference on Parallel and Distributed Processing Techniques and Applications, pp. 399-405 (2004)
8. Unser, M.: Splines: a perfect fit for signal and image processing. IEEE Signal Process. Mag. **16**(6), 22–38 (1999)
9. Unser, M., Aldroubi, A., Eden, M.: B-spline signal processing. IEEE Trans. Signal Process. **41**, 821–848 (1993)
10. Unser, M.: Fast B-spline transforms for continuous image representation and interpolation. IEEE Trans. Pattern Anal. Mach. Intell. **13**, 277–285 (1991)
11. Van De Ville, D., Blu, T., Unser, M., Philips, W., Lemahieu, I., Van De Walle, R.: Hex-spline: a novel family for hexagonal lattices. IEEE Trans. Image Process. **13**(6), 758–772 (2004)
12. Condat, L., Van De Ville, D.: Quasi-interpolating spline models for hexagonally-sampled data. IEEE Trans. Image Process. **16**(5), 1195–1206 (2007)
13. Faille, F., Petrou, M.: Invariant image reconstruction from irregular samples and hexagonal grid splines. J. Image Vis. Comput. **28**(8), 1173–1183 (2010)
14. Thiem, J., Hartmann, G.: Biology-inspired design of digital Gabor filters upon a hexagonal sampling scheme. In: Proceedings of the IEEE International Conference on Pattern Recognition (2000)
15. Jones, J.P., Palmer, L.A.: An evaluation of the two-dimensional gabor filter model of simple receptive fields in cat striate cortex. J. Neurophysiol. **58**(6), 1223–1258 (1987)
16. Xu, Y., Zhang, X.: Gabor Filter bank and its application in the fingerprint texture analysis. In. Proceedings of the Sixth International Conference on Parallel and Distributed Computing Applications and Technologies pp. 829–831 (2005)
17. Huang, L., Shimizu, A., Kobatake, H.: Classification-based face detection using Gabor filter features. In: Proceedings of the IEEE International Conference on Automatic Face and Gesture Recognition, pp. 397–402 (2004)
18. Jain, A.K., Prabhakar, S., Hong, L., Pankanti, S.: Filter bank-based fingerprint matching. IEEE Trans. Image Process. **9**(5), 846–859 (2000)
19. Manjunath, B.S., Ma, W.Y.: Texture features for browsing and retrieval of image data. IEEE Trans. Pattern Analy. Mach. Intell. **18**(8), 837–842 (1996)
20. Veni, S., Narayanankutty, K.A.: Gabor functions for interpolation on hexagonal lattice. J. Electron. Commun. Technol. IJECT **2**(1), 15–19 (2011)
21. Veni, S., Narayanankutty, K.A.: Image enhancement of medical images using Gabor filter bank on hexagonal sampled grids. WASET J. **65**, 816–821 (2010) http://www.waset.org/journals/waset/v65.php
22. Perona, P., Malik, J.: Scale-space and edge detection using anisotropic diffusion. IEEE Trans. Pattern Anal. Mach. Intell. **12**(7), 629–639 (1990)
23. Parker, A., Kenyon, R.V., Troxel, D.E.: Comparison of interpolating methods for image resampling. IEEE Trans. Med. Imaging **MI-2**(1), 31–39 (1983)
24. Thévenaz, P., Blu, T., Unser, M.: Interpolation revisited. IEEE Trans. Med. Imag. **19**(7), 739–758 (2000)
25. Robinson, M.D., Farsiu, S., Lo, J.Y., Toth, C.A.: Efficient restoration and enhancement of super-resolved X-ray images. In: IEEE Proceedings of the International Conference on Image Processing (ICIP) , pp. 629–632 (2008)
26. Destobbeleire. R.: Super-Resolution. Report during Training period at the IMPA, supervised by Velho, L. (IMPA, Brazil) and Mallat, S. (École polytechnique, France) (2002)
27. Lindenbaum, M., Fischer, M., Bruckstein, A.M.: On Gabor's contribution to image enhancement. Pattern Recognit. **27**(1), 1–8 (1994)
28. Zhao, F., Gao, Q.-W., Zhang, D.-X., Lu, Y.-X.: Medical X-ray image enhancement based on Kramer's PDE model. J. Electron. Sci. Technol. China **5**(2), 187–190 (2007)
29. Öktem, H., Egiazarian, K., Niittylahti, J., Lemmetti, J.: An approach to adaptive enhancement of diagnostic X-ray images. EURASIP J. Appl. Signal Process. **5**, 430–436 (2003)
30. Forster, B., Blu, T., Unser, M.: Complex B-splines. Appl. Comput. Harmon. Anal. **20**(2), 261–282 (2006)
31. Chaudhury, K.N., Unser, M.: Construction of Hilbert transform pairs of wavelet bases and Gabor-like transforms. IEEE Trans. Signal Process. **57**(9), 3411–3425 (2009)
32. Tsai, D-Y., Kojima, K.: Wavelet Coefficient mapping for enhancement of chest X-ray images. In: Proceedings, XVII IMEKO World Congress, Dubrovnik, Croatia (2003)
33. Tateyama, T., Nakao, Z., Han, X., Chen, Y.-W.: Contrast enhancement of MR brain images by canonical correlations based kernel independent component analysis. J. Innov. Comput. Inf. Control **5**(7), 1857–1866 (2009)
34. Najim, M. (2007) Digital Filters Design for Signal and Image Processing. ISTE Ltd, USA
35. Periaswamy, S.: Detection of micro calcifications in mammograms using hexagonal wavelets. Thesis work, University of South Carolina (1996)
36. Yang, Y., Li, B.: Non-linear image enhancement for digital TV applications using Gabor filters. In: Proceedings of the IEEE International Conference on Multimedia and Expo, pp. 1018–1021 (2005)
37. Grossberg, S., Mingolla, E., Williamson, J.: Synthetic aperture radar processing by a multiple scale neural system for boundary and surface representation. IEEE Trans. Neural Netw. **8**, 1005–1028 (1995)